Biomedical Optics EXPRESS

Measurements of extrinsic fluorescence in Intralipid and polystyrene microspheres

Vinh Nguyen Du Le,[1] Zhaojun Nie,[2] Joseph E. Hayward,[1] Thomas J. Farrell,[1] and Qiyin Fang[2,3,*]

[1]*Medical Physics and Applied Radiation Sciences, McMaster University, Hamilton, Ontario, Canada*
[2]*School of Biomedical Engineering, McMaster University, Hamilton, Ontario, Canada*
[3]*Department of Engineering Physics, McMaster University, Hamilton, Ontario, Canada*
**qiyin.fang@mcmaster.ca*

Abstract: The fluorescence of Intralipid and polystyrene microspheres with sphere diameter of 1 μm at a representative lipid and microsphere concentration for simulation of mucosal tissue scattering has not been a subject of extensive experimental study. In order to elucidate the quantitative relationship between lipid and microsphere concentration and the respective fluorescent intensity, the extrinsic fluorescence spectra between 360 nm and 650 nm (step size of 5 nm) were measured at different lipid concentrations (from 0.25% to 5%) and different microsphere concentrations (0.00364, 0.0073, 0.0131 spheres per cubic micrometer) using laser excitation at 355 nm with pulse energy of 2.8 μJ. Current findings indicated that Intralipid has a broadband emission between 360 and 650 nm with a primary peak at 500 nm and a secondary peak at 450 nm while polystyrene microspheres have a single peak at 500 nm. In addition, for similar scattering properties the fluorescence of Intralipid solutions is approximately three-fold stronger than that of the microsphere solutions. Furthermore, Intralipid phantoms with lipid concentrations ~2% (simulating the bottom layer of mucosa) produce up to seven times stronger fluorescent emission than phantoms with lipid concentration ~0.25% (simulating the top layer of mucosa). The fluoresence decays of Intralipid and microsphere solutions were also recorded for estimation of fluorescence lifetime.

OCIS codes: (170.3650) Lifetime-based sensing; (170.6280) Spectroscopy, fluorescence and luminescence.

References and links

1. R. Siegel, E. Ward, O. Brawley, and A. Jemal, "Cancer statistics, 2011: the impact of eliminating socioeconomic and racial disparities on premature cancer deaths," CA Cancer J. Clin. **61**(4), 212–236 (2011).
2. M. Müller and B. H. Hendriks, "Recovering intrinsic fluorescence by Monte Carlo modeling," J. Biomed. Opt. **18**(2), 027009 (2013).
3. K. Vishwanath and M. A. Mycek, "Time-resolved photon migration in bi-layered tissue models," Opt. Express **13**(19), 7466–7482 (2005).
4. Q. Wang, K. Shastri, and T. J. Pfefer, "Experimental and theoretical evaluation of a fiber-optic approach for optical property measurement in layered epithelial tissue," Appl. Opt. **49**(28), 5309–5320 (2010).
5. R. Drezek, K. Sokolov, U. Utzinger, I. Boiko, A. Malpica, M. Follen, and R. Richards-Kortum, "Understanding the contributions of NADH and collagen to cervical tissue fluorescence spectra: modeling, measurements, and implications," J. Biomed. Opt. **6**(4), 385–396 (2001).
6. S. K. Chang, D. Arifler, R. Drezek, M. Follen, and R. Richards-Kortum, "Analytical model to describe fluorescence spectra of normal and preneoplastic epithelial tissue: comparison with Monte Carlo simulations and clinical measurements," J. Biomed. Opt. **9**(3), 511–522 (2004).
7. Y. Chen, A. D. Aguirre, P.-L. Hsiung, S. Desai, P. R. Herz, M. Pedrosa, Q. Huang, M. Figueiredo, S. W. Huang, A. Koski, J. M. Schmitt, J. G. Fujimoto, and H. Mashimo, "Ultrahigh resolution optical coherence tomography of Barrett's esophagus: preliminary descriptive clinical study correlating images with histology," Endoscopy **39**(7), 599–605 (2007).
8. V. N. Le, Q. Wang, J. C. Ramella-Roman, and T. J. Pfefer, "Monte Carlo modeling of light-tissue interactions in narrow band imaging," J. Biomed. Opt. **18**(1), 010504 (2013).
9. K. Hazen, J. Welch, S. Malin, T. Ruchti, A. Lorenz, T. Troy, S. Thennadil, and T. Blank, "A Human Tissue Surrogate," WIPO Patent 2001058344 (2001).

#207601 - $15.00 USD Received 5 Mar 2014; revised 27 May 2014; accepted 16 Jul 2014; published 22 Jul 2014

10. A. K. Dunn, V. P. Wallace, M. Coleno, M. W. Berns, and B. J. Tromberg, "Influence of optical properties on two-photon fluorescence imaging in turbid samples," Appl. Opt. **39**(7), 1194–1201 (2000).
11. J. Swartling, J. Svensson, D. Bengtsson, K. Terike, and S. Andersson-Engels, "Fluorescence spectra provide information on the depth of fluorescent lesions in tissue," Appl. Opt. **44**(10), 1934–1941 (2005).
12. S. H. Chung, A. E. Cerussi, S. I. Merritt, J. Ruth, and B. J. Tromberg, "Non-invasive tissue temperature measurements based on quantitative diffuse optical spectroscopy (DOS) of water," Phys. Med. Biol. **55**(13), 3753–3765 (2010).
13. G. Wagnières, S. Cheng, M. Zellweger, N. Utke, D. Braichotte, J. P. Ballini, and H. van den Bergh, "An optical phantom with tissue-like properties in the visible for use in PDT and fluorescence spectroscopy," Phys. Med. Biol. **42**(7), 1415–1426 (1997).
14. B. W. Pogue and M. S. Patterson, "Review of tissue simulating phantoms for optical spectroscopy, imaging and dosimetry," J. Biomed. Opt. **11**(4), 041102 (2006).
15. B. S. Suresh Anand and N. Sujatha, "Effects of Intralipid-10% in fluorescence distortion studies on liquid-tissue phantoms in UV range," J. Biophotonics **4**(1-2), 92–97 (2011).
16. N. Rajaram, T. H. Nguyen, and J. W. Tunnell, "Lookup table-based inverse model for determining optical properties of turbid media," J. Biomed. Opt. **13**(5), 050501 (2008).
17. N. Rajaram, T. J. Aramil, K. Lee, J. S. Reichenberg, T. H. Nguyen, and J. W. Tunnell, "Design and validation of a clinical instrument for spectral diagnosis of cutaneous malignancy," Appl. Opt. **49**(2), 142–152 (2010).
18. Q. Liu, C. Zhu, and N. Ramanujam, "Experimental validation of Monte Carlo modeling of fluorescence in tissues in the UV-visible spectrum," J. Biomed. Opt. **8**(2), 223–236 (2003).
19. Q. Wang, D. Le, J. Ramella-Roman, and J. Pfefer, "Broadband ultraviolet-visible optical property measurement in layered turbid media," Biomed. Opt. Express **3**(6), 1226–1240 (2012).
20. S. L. Jacques, "Optical properties of biological tissues: a review," Phys. Med. Biol. **58**(11), R37–R61 (2013).
21. M. Godin, A. K. Bryan, T. P. Burg, K. Babcock, and S. R. Manalis, "Measuring the mass, density, and size of particles and cells using a suspended microchannel resonator," Appl. Phys. Lett. **91**(12), 123121 (2007).
22. S. Stankovich, D. A. Dikin, G. H. Dommett, K. M. Kohlhaas, E. J. Zimney, E. A. Stach, R. D. Piner, S. T. Nguyen, and R. S. Ruoff, "Graphene-based composite materials," Nature **442**(7100), 282–286 (2006).
23. L. V. Wang and H. I. Wu, *Biomedical Optics: Principles and Imaging* (Wiley, 2007), Chap. 2.
24. P. D. T. Huibers, "Models for the wavelength dependence of the index of refraction of water," Appl. Opt. **36**(16), 3785–3787 (1997).
25. X. Quan and E. S. Fry, "Empirical equation for the index of refraction of seawater," Appl. Opt. **34**(18), 3477–3480 (1995).
26. X. Ma, J. Q. Lu, R. S. Brock, K. M. Jacobs, P. Yang, and X. H. Hu, "Determination of complex refractive index of polystyrene microspheres from 370 to 1610 nm," Phys. Med. Biol. **48**(24), 4165–4172 (2003).
27. S. A. Prahl, "Mie Scattering Calculator". *http://omlc.ogi.edu/calc/mie_calc.html*
28. Z. Nie, R. An, J. E. Hayward, T. J. Farrell, and Q. Fang, "Hyperspectral fluorescence lifetime imaging for optical biopsy," J. Biomed. Opt. **18**(9), 096001 (2013).
29. Y. Yuan, J.-Y. Hwang, M. Krishnamoorthy, J. Ning, Y. Zhang, K. Ye, R. C. Wang, M. J. Deen, and Q. Fang, "High throughput AOTF-based time-resolved fluorescence spectrometer for optical biopsy," Opt. Lett. **34**(7), 1132–1134 (2009).
30. H. J. van Staveren, C. J. Moes, J. van Marie, S. A. Prahl, and M. J. van Gemert, "Light scattering in Intralipid-10% in the wavelength range of 400-1100 nm," Appl. Opt. **30**(31), 4507–4514 (1991).
31. S. T. Flock, S. L. Jacques, B. C. Wilson, W. M. Star, and M. J. van Gemert, "Optical properties of Intralipid: a phantom medium for light propagation studies," Lasers Surg. Med. **12**(5), 510–519 (1992).
32. B. Aernouts, E. Zamora-Rojas, R. Van Beers, R. Watté, L. Wang, M. Tsuta, J. Lammertyn, and W. Saeys, "Supercontinuum laser based optical characterization of Intralipid® phantoms in the 500-2250 nm range," Opt. Express **21**(26), 32450–32467 (2013).
33. J. R. Lakowicz, *Principles of Fluorescence Spectroscopy* (Springer, 2006), Chap. 4.
34. M. Y. Berezin and S. Achilefu, "Fluorescence lifetime measurements and biological imaging," Chem. Rev. **110**(5), 2641–2684 (2010).
35. A. Kienle, L. Lilge, M. S. Patterson, R. Hibst, R. Steiner, and B. C. Wilson, "Spatially resolved absolute diffuse reflectance measurements for noninvasive determination of the optical scattering and absorption coefficients of biological tissue," Appl. Opt. **35**(13), 2304–2314 (1996).
36. M. Gao, G. Lewis, G. M. Turner, A. Soubret, and V. Ntziachristos, "Effects of background fluorescence in fluorescence molecular tomography," Appl. Opt. **44**(26), 5468–5474 (2005).

1. Introduction

Mucosal tissues in the oral cavity, pharynx, esophagus, and digestive system are targets of mucosal cancer, which is responsible for approximately 200,000 deaths annually in the United States [1]. Various optical biopsy methods have been investigated as potential minimally-invasive techniques for early diagnosis and treatment [2–4]. In these studies, phantoms simulating key tissue optical properties (e.g. absorption and scattering coefficients) are extensively used in developing theoretical models [2–4]. Mucosal tissues have two distinguished layers – the epithelium on top of the stromal layer [5,6]. The reduced-scattering coefficients (μ_s') of the stromal layer is about 6-fold higher than that of the epithelium [5,6].

#207601 - $15.00 USD Received 5 Mar 2014; revised 27 May 2014; accepted 16 Jul 2014; published 22 Jul 2014

The epithelial layer thickness is approximately 300 μm [7], which is only a small fraction of the bottom layer thickness [7,8]. Therefore, simulating scattering of the stromal layer of the mucosa is important in optical phantoms which attempt to mimic mucosal tissues.

Intralipid® 10% (defined as: 10 grams of lipids per 100 ml of suspension solution) is commercially available from Fresenius Kabi (Uppsala, Sweden) and Kabivitrum (Stockholm, Sweden) [9]. Dilution of stock Intralipid has been used to simulate tissue scattering in optical phantoms due to the resemblance of its reduced scattering spectrum to that of human tissues, its low absorption [10–13], and its low cost [14]. In many studies, the fluorescence of Intralipid was assumed to be small or negligible in the visible region (350-650 nm) [11–13]. On the other hand, Pogue and Patterson [14] suggested that the lipid content of Intralipid phantoms is likely to fluoresce in the visible region when illuminated with ultraviolet excitation. Anand *et al.* reported that the fluorescence of Intralipid with lipid concentration bellow 0.25% *v*/*v* is significant between 390 and 420 nm when they attempted to use Intralipid as the background scattering to measure the time-resolved fluorescent spectrum of tyrosine dye (emission peak at 300 nm) [15]. Therefore, the endogenous fluorescence of Intralipid is likely to interfere with diffuse reflection measurements in phantom studies and thus influence the prediction of optical properties. However, because of the low concentration of lipid (below 0.25%, notation "*v*/*v*" is omitted in further discussion of intralipid) used in the previous study [15], the simulated scattering of the phantoms was much lower than scattering of human tissue, especially the mucosal tissues. In order to produce Intralipid phantoms simulating mucosa scattering, lipid concentrations of above 1.5% (1.5 grams of lipids per 100 ml of suspension solution) should be used.

Polybead microspheres with sphere diameter of 1 μm are the other common choice for simulating tissue scattering [16–19]. These spheres were preferred not only due to their similar scattering to that of tissues but also their well-controlled size and index of refraction, and their excellent agreement of scattering properties with Mie's theory [16–18]. A previous study using fiber optics spectroscopy claims that fluorescence of microsphere (diameter of 1 μm) phantoms with concentration of 0.72% (defined as 0.72 gram of particles per 100 ml suspension solution, corresponding to approximately 0.0131 spheres per cubic micron) after mixing with hemoglobin solution is small and negligible [19]. However, hemoglobin strongly absorbs photons in the visible region, and fluorescence signal from this region might not be detected.

While matching Intralipid and polystyrene microspheres scattering to tissue scattering is certainly a key requirement in the fabrication of optical phantoms for fluorescence and diffuse reflection studies, the assumption that their fluorescence is small and can be neglected has not been rigorously validated. The purpose of this study is to establish the fluorescence profile of both Intralipid and polystyrene microspheres in optical phantom studies for the broadband spectral region 360-650 nm by separately evaluating the fluorescent intensity of the Intralipid and microsphere phantoms at concentrations that mimic tissue scattering. This was achieved by performing fluorescence spectroscopy of the phantoms using an optical fiber coupled with a spectrometer. In addition, the fluorescence decays of these phantoms were measured with a time-resolved fluorescence spectroscopy system and the average fluorescence lifetime was retrieved for comparison with that of other fluorescent dyes of biological importance.

2. Methods

2.1 Intralipid phantoms

Three sets of seven Intralipid phantoms (total of 21 phantoms) with concentrations of 0.25%, 0.5%, 1%, 1.5%, 2%, 3% and 5% were created for fluorescence measurements. These phantoms were prepared by diluting the concentrated Intralipid® 20% solution (manufactured by Fresenius Kabi, Uppsala, Sweden and distributed by Baxter Healthcare Corp., Deerfield, IL) in de-ionized water. The volume of each phantom was 10 ml which was contained within 12 ml test tubes. A separate set of phantoms with much lower lipid concentration 0.05% - 0.25% was also prepared for transmission measurements using a collimated xenon lamp light

#207601 - $15.00 USD Received 5 Mar 2014; revised 27 May 2014; accepted 16 Jul 2014; published 22 Jul 2014

source from a spectrometer (Ultraspec 3000, Pharmacia Biotech Inc., NJ). The transmission data (T) were used to calculate scattering coefficients (μ_s) by applying the relationship $\mu_S = -\ln(T)/L$, where L = 1 mm is the path length of the quartz cuvette used [20]. The measurements allowed extrapolation of μ_s for phantoms with higher lipid concentration

2.2 Microsphere phantoms and Mie theory

Three microsphere phantoms with concentrations of 0.72%, 0.4%, 0.2% solids *w*/*v* aqueous suspension were prepared by diluting the 2.5% (the notation of *w*/*v* is omitted in further discussion of microspheres) stock solution of 1 μm diameter polystyrene microspheres (Polysciences Inc., Warrington, PA). The corresponding number of spheres per cubic micrometer in these phantoms is 0.0131, 0.0073, 0.00364 which were found by applying the relationship in Eq. (1). In this equation, N is number of spheres per cubic micrometer, x is particle concentration in gram per milliliter (x = 0.0072, 0.004, 0.002 *g*/ml, respectively), y = 1.05 *g*/*ml* is the density of polystyrene [21,22], and d = 1 μm diameter of sphere in micrometers.

$$N = \frac{6x}{y\pi d^3} \tag{1}$$

Mie theory was used to calculate the scattering coefficients of the microsphere phantoms in the wavelength region 350-650 nm. The numerical calculations for the Mie theory was performed using MATLAB® (Mathworks, Natick, MA) routine which was described elsewhere [23]. This particular script can only perform single wavelength calculations; however, a simple modification was added to enable multi-wavelengths calculations by incorporating the wavelength dependent characteristics of the index of refraction of water and of the microspheres. The index of refraction of water, n_{water} was calculated using Eq. (2) which was derived in previous studies [24, 25]. In Eq. (2), λ is the wavelength in nanometers.

$$n_{water}(\lambda) = 1.313 + \frac{15.762}{\lambda} - \frac{4382}{\lambda^2} + \frac{1145500}{\lambda^3} \tag{2}$$

The index of refraction of the polystyrene microspheres, n_{sphere}, was calculated using the Cauchy dispersion relation as shown in Eq. (3) which was derived by Ma *et al*. [26] In Eq. (3), λ is the wavelength in micrometers.

$$n_{sphere}(\lambda) = 1.5725 + \frac{0.0031080}{\lambda^2} - \frac{0.00034779}{\lambda^4} \tag{3}$$

As a verification of the program, the reduced scattering coefficients for microsphere phantom 0.72% were also calculated with Prof. Prahl's Mie calculator [27]. Since Prof. Prahl's calculator can only perform single wavelength calculations, the comparison with current program was performed at wavelengths with step of 25 nm.

2.3 Instruments

Fluorescence measurements of the Intralipid phantoms were performed using an excitation pulsed laser at 355 nm (PNV-001525-140, Teem Photonics, Meylan, France), a single optical fiber with core diameter of 600 μm and numerical aperture of 0.12 for illumination and detection, a calibrated spectrometer (UV-NIR-200, StellarNet Incorporation, Tampa, FL) to record fluorescence at a broadband wavelength range 350-650 nm, and a calibrated acousto-optic-tunable-filter (AOTF) -based time-resolved spectrometer for estimation of lifetime and verification of fluorescence signals. Details of the time-resolved system can be found elsewhere [28,29]. The advantage of using excitation wavelength at 355 nm in tissue is that most of biological fluorophores such as NADH, collagen, and elastin, etc. can be excited at this wavelength to emit light in visible region.

#207601 - $15.00 USD Received 5 Mar 2014; revised 27 May 2014; accepted 16 Jul 2014; published 22 Jul 2014

In all phantom measurements, the fiber tip was held perpendicular to the phantom surface and was immersed within the phantoms at a depth of approximately 2 mm from the surface. The laser power was set at approximately 2.8 μJ and the integrating time of the spectrometer was set at 0.75 second. These values were chosen to maintain good signal for observation while avoiding spectrometer saturation. Background fluorescence was also taken into account by subtracting fluorescence of the phantoms from that of test tube filled with only de-ionized water.

3. Results

3.1 Scattering of phantoms compared to mucosal tissues

The linear relationship between lipid concentration and μ_s with R-squared values within range of 0.97 and 0.99 was obtained for all wavelengths within 350-650 nm. Figure 1(a) shows examples of linear regressions at 450 nm and 500 nm with R-squared values of 0.98.

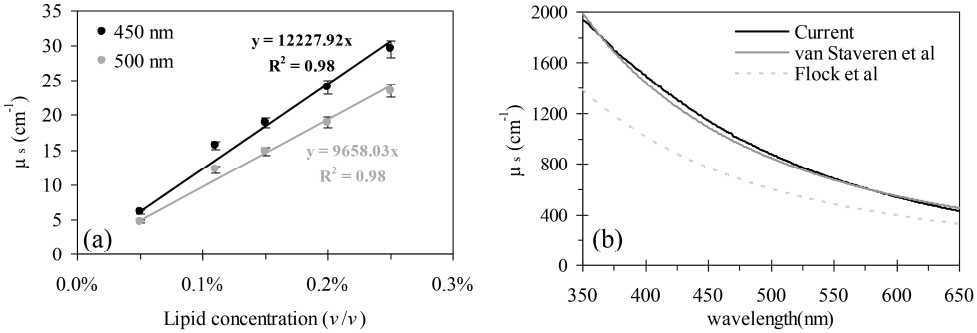

Fig. 1. (a) Scattering coefficients (μ_s) as a function of lipid concentration at 450 nm and 500 nm, (b) Predicted μ_s of Intralipid 10%: extrapolated data (current) *vs.* previous literature data by van Staveren et al [30] and Flock et al. [31].

The μ_s values of Intralipid 10% was extrapolated using a linear regression method and was compared to previous data reported by van Staveren *et al*. [30] and by Flock *et al*. [31] (Fig. 2). As shown in Fig. 1(b), an agreement (within 10% error) in μ_s values between extrapolated data and the data from van Staveren *et al.* [30] was obtained. Our method of measuring Intralipid's scattering coefficients is similar to that of van Staveren et al. [30]. However, the main difference is that the current transmission measurement was performed over broadband wavelength range 350-650 nm with 1-mm-thick quartz cuvette while van Staveren et al's transmission measurement was performed with lasers (457.9, 514.5, 632.8 and 1064 nm) and 3.55-mm-thick glass cuvette. Therefore, the current method did not require fitting assumption to obtain the scattering spectrum and was able to measure transmission of solution with higher lipid concentration. The current prediction of μ_s of Intralipid 10% was also in agreement with Aernout et al's prediction which applied invert adding doubling (IAD) method to predict bulk optical properties from the integrating sphere measurement of total transmission and total reflection from thin slabs [32]. In van Staveren's study, anisotropy (g) was calculated as $g = 1.1 - (0.00058)\,\lambda$, where λ is wavelength in nanometers [30]. In this study, a similar calculation was applied to obtain μ_s' values for Intralipid phantoms from the measured and extrapolated μ_s values.

Comparing with previously reported μ_s' values of mucosal tissue [5,6], it was shown that Intralipid phantoms with lipid concentrations between 0.25% and 0.5% are best for simulation of epithelial scattering while those with lipid concentration between 1.5% and 2% are best for simulation of stromal scattering (Fig. 2). Phantoms with lipid concentration 3% and 5% were also produced to further observe the fluorescence trend at high μ_s' values.

#207601 - $15.00 USD Received 5 Mar 2014; revised 27 May 2014; accepted 16 Jul 2014; published 22 Jul 2014

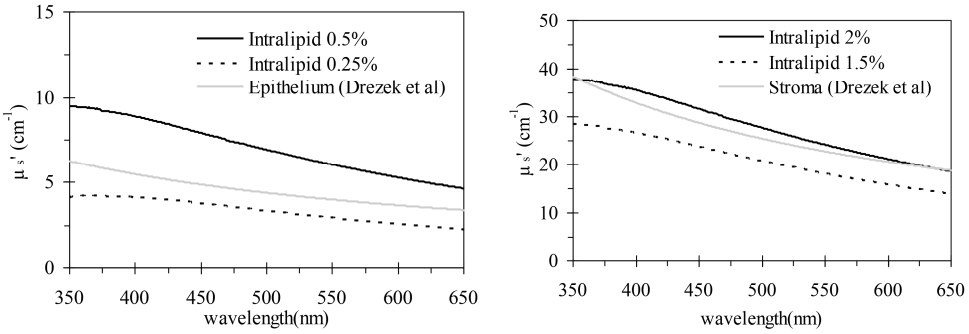

Fig. 2. Reduced-scattering coefficients (μ_s'): Intralipid phantoms at different lipid concentration versus literature data [5].

Figure 3 compares the current numerical calculation to Prof. Prahl' calculator for scattering coefficients μ_s of microsphere phantom 0.72% (Fig. 3(a)) and the sphere's anisotropy values g (Fig. 3(b)). An excellent agreement between the two programs with average percentage error less than 0.1% was obtained. As shown in Fig. 3(b), the anisotropy of 1 μm microsphere is within range of 0.88-0.93 with the peak at around 475 nm.

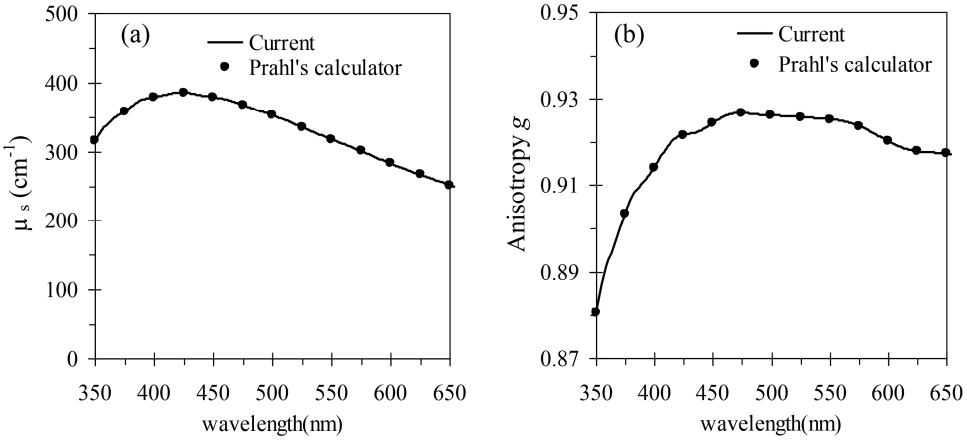

Fig. 3. Numerical calculation of Mie theory using current program compared to Prahl's calculator [27]: (a) scattering coefficients of 0.72% microsphere phantom, (b) anisotropy.

Figure 4 shows the calculated reduced scattering coefficients μ_s' for all microsphere phantoms used. The μ_s' values for mucosal tissues were also plotted in the same graph for comparison. As shown in Fig. 4, microsphere 0.72% is optimum for simulation of stromal scattering. The resulted spectrum also agrees with previous experimental measurements with optical fiber spectroscopy and neural networks [19]. The advantage of the current approach over Prof. Pralh's calculator is the ability to calculate broadband spectrum of μ_s and anisotropy g with single input of sphere concentration and sphere diameter. Therefore, the current method was able to perform fast calculation of μ_s' of the microsphere phantoms over broadband wavelength range 350-650 nm without using fitting approach (Fig. 4).

#207601 - $15.00 USD Received 5 Mar 2014; revised 27 May 2014; accepted 16 Jul 2014; published 22 Jul 2014

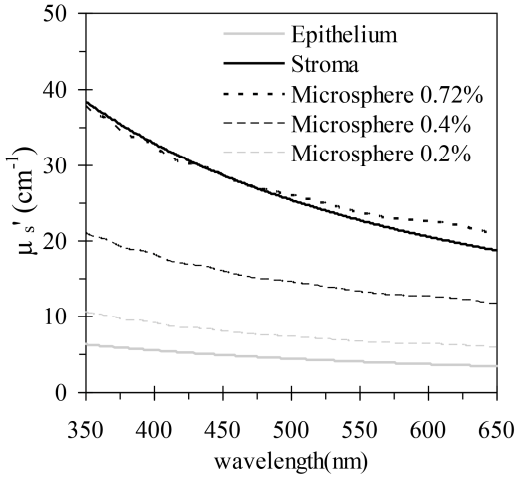

Fig. 4. Calculated reduced scattering coefficients (μ_s') of microsphere phantoms versus μ_s' of mucosal tissues.

3.2 Fluoresence of Intralipid and of microsphere phantoms

The fluorescent intensity spectrum of Intralipid phantoms collected with the spectrometer between 360 and 650 nm is shown in Fig. 5. Background fluorescence was taken into account by subtracting fluorescence of the phantoms to that of test tube filled with only de-ionized water. All error bars shown in these graphs were obtained from standard deviation calculation of measurements of different phantoms with respect to a specific lipid concentration. As shown in Fig. 5, the fluorescence generally increases gradually from 360 nm to 450 nm with a peak at around 450 nm, and increases more rapidly from 477 nm to 500 nm with a peak at 500 nm. Fluorescence decreases quickly from 525 nm to 650 nm (Fig. 5). In these results, the excitation wavelength is not seen because dichroic mirror and filter were used to block back scattered excitation light [28,29].

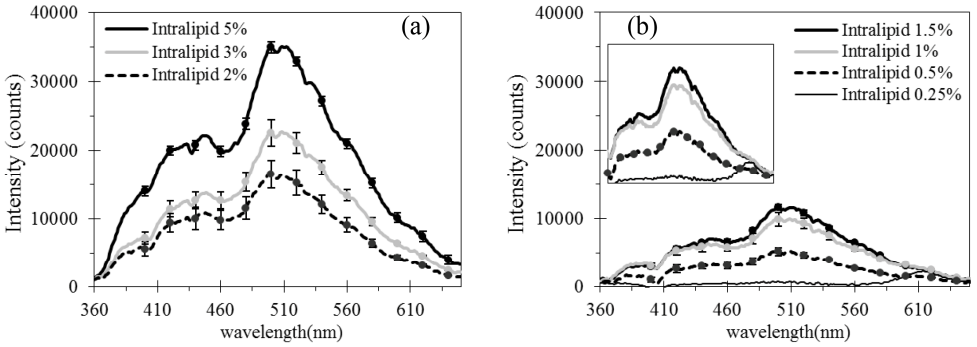

Fig. 5. Fluorescent intensity of Intralipid phantoms with different lipid concentrations: 2%, 3%, 5% (a), 0.25%, 0.5%, 1%, and 1.5% (b). The inset in (b) shows auto-scales of the same curves.

Figure 5 also shows that increasing lipid concentration from 0.25% to 2% increases fluorescent signals up to seven-fold (14-fold for lipid concentrations up to 5%). To validate the results from the spectrometer, the AOTF time-resolved fluorometer was also used to obtain fluorescent spectra of the lipid phantoms in the wavelength range 400-480 nm. As shown in Fig. 6, the trends in the fluorescence emission spectrum from the time-resolved fluorometer is in good agreement with the spectrometer measurements so that lipid 5% produced maximum fluorescent intensity, followed by lipid 3%, 2% and so on .

#207601 - $15.00 USD Received 5 Mar 2014; revised 27 May 2014; accepted 16 Jul 2014; published 22 Jul 2014

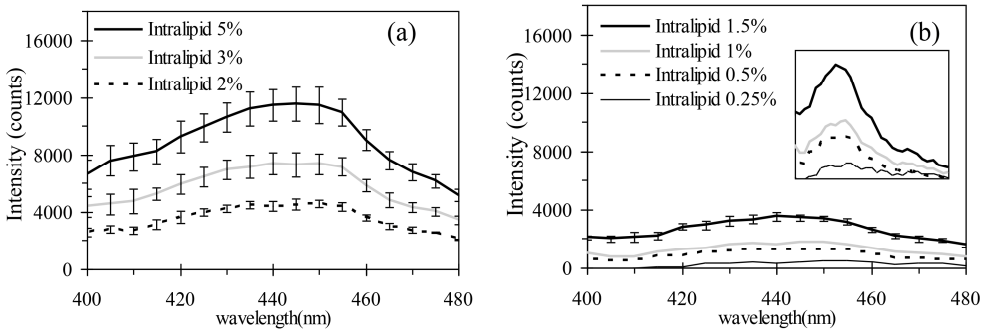

Fig. 6. Fluorescent intensity of Intralipid phantoms with different lipid concentration: 2%, 3%, 5% (a), 0.25%, 0.5%, 1%, 1.5% (b). The inset in (b) shows auto-scales of the same curves. Data was collected with a time-resolved fluorometer.

Fluorescent intensity at 450 nm as function of lipid concentration (or reduced scattering coefficients) collected with both systems is plotted on the same graph in Fig. 7 for demonstration. In Fig. 7, the fluorescent intensity at 450 nm of the Intralipid phantoms was normalized to that of the Intralipid 5% phantom when using the spectrometer and the AOTF time-resolved fluorometer, respectively.

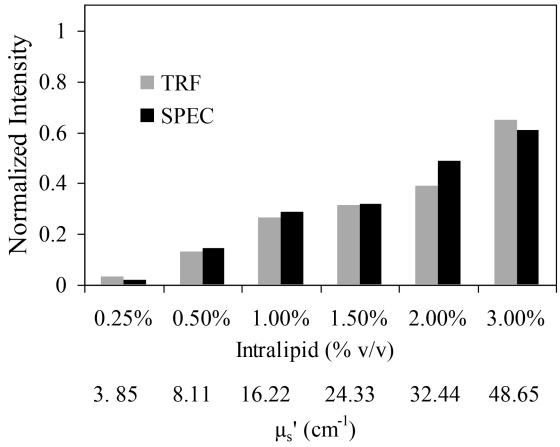

Fig. 7. Fluorescent intensity collected with a time-resolved fluorometer (TRF) and spectrometer (SPEC) at 450 nm as a function of lipid concentration or μ_s' values at 450 nm. Intensity of phantoms in each case was normalized to that of phantom with lipid concentration 5%.

Figure 8 shows the fluorescent intensity of the microsphere phantoms measured with the spectrometer (Fig. 8(a)) and with the time-resolved fluorometer (Fig. 8(b)). Again, a trend agreement was obtained with both methods so that maximum fluorescent intensity was obtained with microsphere concentration of 0.72% (0.0131 sphere per cubic micron) followed by microsphere concentration of 0.4% (0.0073 sphere per cubic micron). The main peak in microsphere fluorescence was seen at 500 nm and is more pronounced at the highest sphere concentration at 0.72% (Fig. 8(a)).

#207601 - $15.00 USD Received 5 Mar 2014; revised 27 May 2014; accepted 16 Jul 2014; published 22 Jul 2014

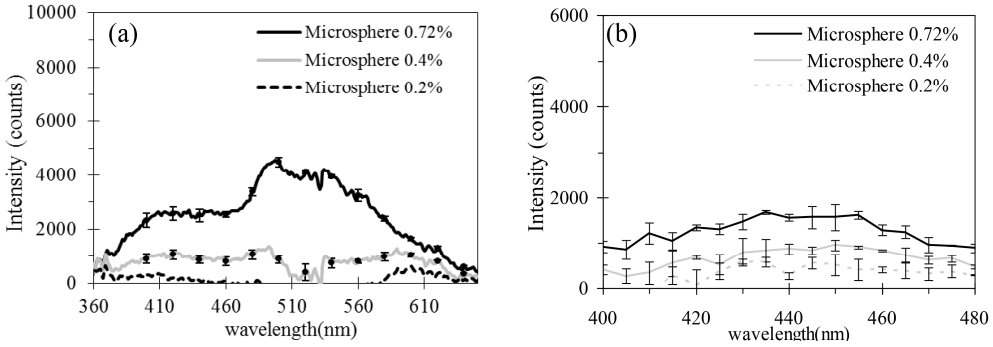

Fig. 8. Fluoresence of microsphere phantoms using a spectrometer (a), and a time-resolved fluorometer (b).

However, the fluorescent intensity of the 0.72% microsphere phantom is much smaller than that of the 2% Intralipid phantom (Fig. 9) while both have similar scattering to that of the stromal layer (Fig. 2 and Fig. 4). On average, fluorescence of the 2% Intralipid phantom was approximately 3 times stronger than that of the 0.72% microsphere phantom (Fig. 9). As shown in Fig. 9, even the 1.5% Intralipid phantom which has lower scattering than the 0.72% microsphere, 1.5% Intralipid phantom produces fluorescence signals with intensity approximately twice as strong as the 0.72% microsphere phantom (Fig. 9).

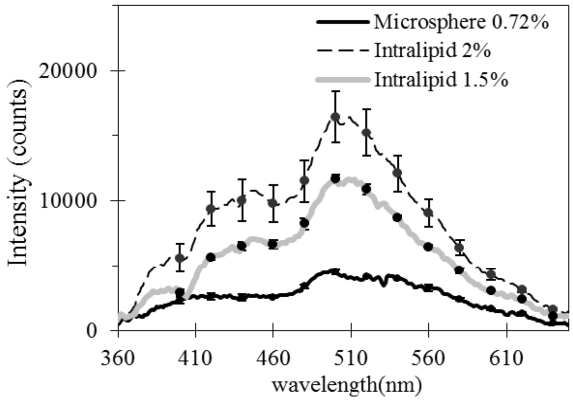

Fig. 9. Fluoresence of Intralipid compared to microspheres: The measurements were performed with a spectrometer.

3.3 Fluoresence decays of Intralipid and of polystyrene microsphere

Fluorescence decays of Intralipid and microsphere phantoms were also recorded with the digitizer for estimation of lifetime. Figure 10 shows examples of the normalized fluorescence decays for phantoms with lipid concentration 2% and microsphere 0.72% at emission peak 455 nm. A bi-exponential deconvolution method was used to retrieve the intrinsic response function from measured fluorescence signals [33]. Based on the fractional contribution of each component [33], an average lifetime of 4.53 ± 0.21 ns and 1.81 ± 0.1 ns was obtained for Intralipid and microspheres, respectively. Similar decays were obtained for phantoms with other lipid and microsphere concentrations. The calculated lifetime (τ) of Intralipid is in the similar range of the lifetime of other visible-emission-dyes used in various fluorescent studies such as Fluorescein (τ = 4 ns), Pyrene (τ = 2.97 ns), 4',6-Diamidino-2-phenylindole or DAPI (τ = 2.78 ns), Rhodamine 123 (τ = 3.97 ns), Alexa 532 (τ = 2.53 ns), and FAD (τ = 2.91 ns) [34]. Therefore, the possibility for Intralipid to interfere with fluorescence measurements of these dyes is high if used together in a tissue phantom.

#207601 - $15.00 USD Received 5 Mar 2014; revised 27 May 2014; accepted 16 Jul 2014; published 22 Jul 2014

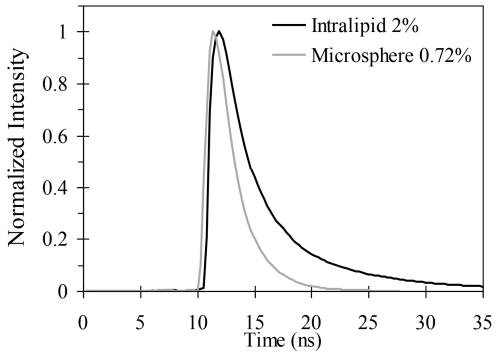

Fig. 10. Normalized fluorescence decays of Intralipid phantoms with lipid concentration of 2% and microsphere phantom with sphere concentration of 0.72%.

4. Conclusions

These measurements have provided a quantitative measurement of fluorescence of Intralipid and polystyrene microspheres (diameter of 1 μm) in the wavelength range 360-650 nm with consideration of microsphere and lipid concentrations that match the reduced-scattering coefficients of human mucosal tissue. It has been shown that Intralipid phantoms have a primary emission peak at 500 nm and a secondary emission peak at 450 nm while microspheres appear to have a single peak around 500 nm. The fluorescence intensity of Intralipid is significantly stronger (average approximately 3-fold) than that of microspheres considering lipid and microsphere concentration at levels which simulate tissue scattering. In addition, the calculated fluorescence lifetime of Intralipid is approximately 2.5 times longer than that of microspheres (4.53 ns vs. 1.81 ns). Most fluorescence dyes used in research strongly fluoresce in region 450-600 nm and have the average life time as close as that of Intralipid. For example, Fluorescein and Rhodamine 123 has strong emission at around 450-500 nm and 520-600 nm, respectively and average life-time of 4 ns and 3.97 ns, respectively [34]. Consequently, the probability for fluorescence of Intralipid to interfere with fluorescence of the studied fluorophore is much higher than that of microspheres. Therefore, the fluorescence of microsphere phantoms might be neglected in optical phantom studies. However, the same assumption may not be accurate in the case of Intralipid phantoms.

In fluorescence studies, background medium consists of pure absorber and pure scatterer which do not fluoresce so that the fluorescence of fluorophore can be studied independently [11–13, 35]. Furthermore, in diffuse reflection studies the reflected light from the phantoms is usually subtracted to background signal collected from DI water or instrument's noise [8,19]. However, this method might introduce error if Intralipid is used as scatterer because it fluoresces strongly, and its fluorescence intensity might not be negligible as previously claimed [31]. Therefore, a careful data processing method such as subtraction of average fluorescence response to raw signal [36] is necessary to correctly analyze optical properties and intrinsic fluorescence of the target fluorophore. Although mimicking tissue scattering with low-cost materials is a key factor in the use of Intralipid phantoms, our measurements indicate that fluorescence of Intralipid with lipid concentrations to mimic stromal scattering (1.5% and 2%) is significant and should not be ignored.

Acknowledgments

The authors would like to thank Prof. Leyla Soleymani of the Department of Engineering Physics at McMaster University for access to her laboratory during phantom fabrication. This project is supported in part by the Natural Sciences and Engineering Research Council (NSERC) of Canada, Canada Foundation for Innovation (CFI), Ontario Ministry of Research and Innovation (MRI), and Canada Canadian Cancer Society Research Institute (CCSRI). QF holds the Canada Research Chair in Biophotonics.